UNIVERSITY OF BIRMINGHAM
University of Birmingham Research at Birmingham

Monte Carlo Model of the Large Modular Array for Positron Emission Particle Tracking

Herald, Matthew; Hampel, Dawid; Wheldon, Tzany Kokalova; Seville, Jonathan; Windows-Yule, Christopher

DOI:
10.1109/ACCESS.2023.3255505

License:
Creative Commons: Attribution (CC BY)

Document Version
Publisher's PDF, also known as Version of record

Citation for published version (Harvard):
Herald, M, Hampel, D, Wheldon, TK, Seville, J & Windows-Yule, C 2023, 'Monte Carlo Model of the Large Modular Array for Positron Emission Particle Tracking', *IEEE Access*, vol. 11, pp. 25982-25990. https://doi.org/10.1109/ACCESS.2023.3255505

Link to publication on Research at Birmingham portal

General rights
Unless a licence is specified above, all rights (including copyright and moral rights) in this document are retained by the authors and/or the copyright holders. The express permission of the copyright holder must be obtained for any use of this material other than for purposes permitted by law.

•Users may freely distribute the URL that is used to identify this publication.
•Users may download and/or print one copy of the publication from the University of Birmingham research portal for the purpose of private study or non-commercial research.
•User may use extracts from the document in line with the concept of 'fair dealing' under the Copyright, Designs and Patents Act 1988 (?)
•Users may not further distribute the material nor use it for the purposes of commercial gain.

Where a licence is displayed above, please note the terms and conditions of the licence govern your use of this document.

When citing, please reference the published version.

Take down policy
While the University of Birmingham exercises care and attention in making items available there are rare occasions when an item has been uploaded in error or has been deemed to be commercially or otherwise sensitive.

If you believe that this is the case for this document, please contact UBIRA@lists.bham.ac.uk providing details and we will remove access to the work immediately and investigate.

Download date: 19. Jul. 2023

IEEE Access
Multidisciplinary | Rapid Review | Open Access Journal

Received 8 December 2022, accepted 4 March 2023, date of publication 10 March 2023, date of current version 17 March 2023.

Digital Object Identifier 10.1109/ACCESS.2023.3255505

APPLIED RESEARCH

Monte Carlo Model of the Large Modular Array for Positron Emission Particle Tracking

MATTHEW HERALD[1], DAWID HAMPEL[2], TZANY KOKALOVA WHELDON[2,3], JONATHAN SEVILLE[1,3], AND CHRISTOPHER WINDOWS-YULE[1,3]

[1]School of Chemical Engineering, University of Birmingham, B15 2TT Birmingham, U.K.
[2]School of Physics and Astronomy, University of Birmingham, B15 2TT Birmingham, U.K.
[3]Positron Imaging Centre, University of Birmingham, B15 2TT Birmingham, U.K.

Corresponding author: Matthew Herald (mxh1092@bham.ac.uk)

This work was supported in part by the Engineering and Physical Science Research Council under Grant EP/T034327/1, and in part by the Advanced Imaging and Numerical Modelling of Segregation and Transport of Plastics in Fluidised Beds: Toward a Circular Economy for Plastics.

ABSTRACT Positron emission particle tracking (PEPT) is a non-invasive technique used to study fluid, granular, and multi-phase systems of interest to academia and industry. PEPT employs position-sensitive radiation detectors to record gamma rays in coincidence and track the movement of discrete sources. A modular detector array, the Large Modular Array (LaMA), has been constructed at the University of Birmingham's Positron Imaging Centre (PIC) to enable custom detector geometries. To estimate the LaMA's performance characteristics prior to experimentation, assist in developing optimised camera geometries, and determine ideal PEPT tracer characteristics a Monte Carlo model of LaMA is created and subsequently validated with experimental measurements. Validation is achieved through comparisons of the spatial resolution and count-rate response following the National Electrical Manufacturers Association (NEMA) industry standard protocol. Notably, the model's pulse-processing chain is autonomously calibrated to match experimental measurements using a recently developed technique which applies an evolutionary algorithm. The results show the simulated spatial resolution of the validated model matches the experiment to within 5%. Additionally, the total, true, and corrupted count-rates are reproduced to a mean error of 3.41%. This calibrated detector model strengthens the PIC's modelling capabilities. To facilitate future research, this model has been made publicly available through the PIC's GitHub repository.

INDEX TERMS Digital twin, GATE, Monte Carlo, positron emission particle tracking.

I. INTRODUCTION

Positron emission particle tracking (PEPT) is an imaging technique used to study opaque engineering and scientific systems using flow-following tracers labelled with positron-emitting radionuclides [1]. Positrons annihilate with electrons in close proximity to the labelled tracer, producing back-to-back 511 keV gamma-rays which can be detected with position-sensitive radiation detectors such as gamma cameras or positron emission tomography (PET) scanners [2]. Reconstruction of the labelled tracer position requires detecting both annihilation photons in coincidence to form a line-of-response (LoR) and applying a PEPT algorithm on a sample of LoRs to find the most likely annihilation point [3]. By detecting the tracer successively, a time-dependent trajectory is developed which can be analysed to determine system properties such fully three-dimensional velocity fields, tracer re-circulation times, and diffusivity [1]. PEPT has been used extensively over the last 30 years to study a variety of equipment ranging from coffee roasters, washing machines, and liquid metal castings [4], [5], [6].

To perform a PEPT measurement, equipment must first be moved to a lab and placed in the field-of-view (FOV) of a position-sensitive detector. At the University of Birmingham's Positron Imaging Centre (PIC), detectors like the ADAC Forte and SuperPEPT have been acquired or built specifically for PEPT measurements [7]. The Forte dual-headed positron camera was acquired because the two

The associate editor coordinating the review of this manuscript and approving it for publication was Giovanni Merlino.

This work is licensed under a Creative Commons Attribution 4.0 License. For more information, see https://creativecommons.org/licenses/by/4.0/

detector heads can be separated up to between 250 mm and 800 mm, which enables the accommodation of a variety of equipment while optimising detector sensitivity. This system can record LoRs up to approximately 100 kHz [8]. Additionally, SuperPEPT, which has recently been constructed using components from CTI/Siemens ECAT EXACT 31, ART, and EXACT HR+ scanners has a cylindrical geometry of about 400 mm in diameter and 544 mm in length. The diameter can be separated up to 600 mm to place an experiment in the FOV, but must be closed again to record data. SuperPEPT records LoRs up to 2500 kHz, a factor of 20 higher than the Forte, enabling improved spatiotemporal resolution of PEPT trajectories [9].

However, there are instances where experimental equipment is too large or consists of awkward geometries which cannot be easily fit into the FOV of existing systems. To address this, a modular detector array, named the Large Modular Array (LaMA), has been designed to be assembled around experimental systems in custom geometries [10]. LaMA consists of building block, called 'boxes', which contain four ECAT951 block detectors. These boxes can be placed in nearly any configuration and connected to a coincidence processor, allowing flexible geometries to be designed for imaging large-scale industrial equipment [11]. Since the LaMA is reconfigured in a different geometry for each experiment, the performance characteristics of the camera are difficult to predict. As such, estimating the spatiotemporal resolution of the expected trajectories, designing an optimised geometry, and selecting an appropriate tracer activity for a given experiment can be challenging.

In this work we describe and validate a Monte Carlo model of the LaMA which will be used to help optimise experiments in the future. This model is created using the Geant4 Application for Tomographic Emission (GATE), a Monte Carlo radiation transport software which emulates the detector geometry, radioactive sources, and electronic pulse-processing of particles interacting with the detector [12], [13]. The performance of the camera in a simple geometry is characterised following the industry-standard National Electrical Manufacturers Association (NEMA) protocol [14]. Notably, the pulse-processing model is calibrated by through a recently developed method which compares the simulated and real performance characteristics and tunes parameters of the pulse-processing model using an evolutionary algorithm [15], [16], [17].

A. THE LARGE MODULAR ARRAY (LaMA)

The idea for the LaMA was developed at the PIC in the early 2000s, growing out of the need to have a detector system which could image large or awkward industrial systems and potentially be able to be transported to equipment which could not be moved. One feature that was identified as being key to this future system was being modular so that custom geometries could be tailored to each experiment. To this end, initially, three CTI/Siemens ECAT ring scanners were acquired and dismantled to retrieve the block detectors which could then be reassembled into a new geometries [10].

Each block detector consists of an 8×8 bismuth germanate (BGO) crystal array, with each crystal measuring 6.25 mm in width, 6.75 mm in height, and 30 mm in thickness. The BGO crystals are optically coupled to a 5 mm thick glass light guide and four photo-multiplier tubes (PMTs), each 100 mm in length. Using the 192 block detectors extracted from the PET scanners, a modular unit consisting of four blocks was designed. Each of these units are termed a 'box' and 48 boxes were constructed in total. Each box is approximately 360 mm in width, 95 mm in height (including spacers), and 460 mm in thickness with each of the four block detectors spaced 90 mm apart from centre-to-centre. A single box is shown on the left side of Fig. 1 and a stack of four boxes is shown on the right. These modular units are the fundamental building blocks of LaMA. Currently, up to 32 boxes can be connected to a single coincidence processor unit to form a detector array. By using more than one coincidence processor and merging the data streams in post-processing, all 48 boxes can be used simultaneously, but coincidences can only be formed between boxes connected to a shared coincidence processor.

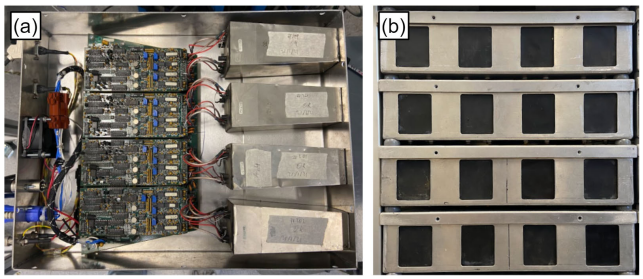

FIGURE 1. (a) A view inside a single box where four block detectors are mounted. (b) A stack of four boxes. The geometry used in this work is two stacks of four boxes separated by 500 mm.

B. Geant4 APPLICATION FOR TOMOGRAPHIC EMISSION (GATE)

GATE is a Monte Carlo radiation transport and detector simulation software designed for emulating the geometries, sources, and pulse-processing chain of imaging systems [12]. Many different types of detectors and imaging modalities have been modelled using GATE, including other detector systems used for PEPT such as the ADAC Forte and Siemens Inveon [13], [18], [19]. GATE is a useful tool for modelling PEPT experiments because it provides output comparable to real detectors and serves as 'sandbox' through which changes in the detector or source properties can be assessed, synthetic data can be processed to verify imaging techniques, or limits of techniques can be investigated without expending the considerable time and resources required for physical experimentation. Of special importance for the model presented in this work, a GATE model of a PEPT detector and experimental geometry can be used to the assess impact of changes in the geometry to the sensitivity of the system and affect this has on

tracer trajectories quantified through estimates of their spatial and temporal resolution [20], [21], [22].

One useful feature of GATE is the 'parameterisation' of the simulation scripts which allows users to quickly change aspects of the simulation through the command line. Using this, the source activity, placement of LaMA's boxes, and the values for parameters of the digitizer can be edited without having to manually change the file. In this work, we use GATE to first replicate the geometry of the LaMA and the source, then calibrate the digitizer through evolutionary an evolutionary algorithm which is able to edit the pulse-processing settings of the detector through parameterised simulation scripts. The fitness of a set of candidate solutions with tune-able digitizer parameters is then compared through the ability of the GATE model to replicate the experimentally measured performance characteristics.

C. EVOLUTIONARY ALGORITHMS

When calibrating simulated models to experimental measurements, the complex relationship between variables, noisy measurements, and the large number of solutions that need to be tried to explore the solution space leads to a difficult optimisation problem with many false local minima [23]. When there are several parameters which need to be optimised, such as encountered in a digitizer model, traditional approaches like design-of-experiments become too unwieldy and gradient-based optimisers struggle to overcome local minima in a multi-dimensional and noisy solution space. This has led most GATE models to be calibrated manually using estimates of the optimal parameters provided by manufacturers of the detectors [24], [25]. This type of manual tuning is both subjective and also not guaranteed to produce the optimal calibration.

However, a type of optimisation algorithm that has been shown to excels in these cases are evolutionary algorithms [15], [26]. Evolutionary algorithms emulate biological evolution by using a group of simulations to act as a population with varied features. In this way, the fitness of individual simulations against a selective pressure can be quantified. To improve the fitness of the next generation of simulations, the fittest simulations are allowed to reproduce which allows their features to be transferred and some random mutations added to increase diversity, potentially introducing beneficial features.

In this work, the Covariance Matrix Adaptation using Evolutionary Strategy (CMA-ES), which is a stochastic optimiser for robust non-linear non-convex numerical optimisation, is used to perform the model calibration [16]. While CMA-ES generates, assesses, and updates solutions to parameters of the digitizer, an additional software is used to couple CMA-ES to the GATE simulation. This software is the Autonomous Characterisation and Calibration via Evolutionary Simulation (ACCES) which is a Python interface to the CMA-ES algorithm specifically designed for general calibration simulations and has been previously used to calibrate a GATE model of the ADAC Forte [15], [17]. More details about our use of this software to calibrate the LaMA digitizer are provided in Section II-C.

II. METHODS

A. CHARACTERISATION EXPERIMENTS

Two sets of characterisation experiments are conducted to measure the spatial resolution and count-rate response of the LaMA in a simple geometry. These two characteristics are the most important detector characteristics in regard to PEPT experiments because spatial resolution predominately influences the ability to resolve a point-like source and the digitizer model controls the count-rate response curve. Thus, these two characteristics ultimately determine the spatial and temporal resolution of a PEPT tracer, which are the characteristics of interest for users of PEPT algorithms [7].

In order to characterise LaMA's performance characteristics, a single, simple geometry was chosen. This geometry is a dual-headed stack of four boxes on either side of a source. The two stacks are separated by 500 mm. This configuration is used because of the low number of boxes required and also because of the large solid angle it creates with the source, allowing three-dimensional tracking of a point source, which is important for PEPT algorithms. Additionally, by choosing a simple geometry and achieving a calibration with the GATE model, it is expected that when the system is scaled up for future experiments the GATE model will remain accurate. The LoRs collected from these experiments are processed according to the NEMA protocol and in all cases the centre of the FOV is defined as 0, 0, 0 mm.

1) SPATIAL RESOLUTION

The spatial resolution of the detector is defined as the full-width half-maximum (FWHM) of the point-spread-function (PSF) for a small point-like source in the detector's FOV. The source used for this experiment is a 1 mm sphere of anionic exchange resin, volumetrically activated with fluorine-18 in a solution of water produced by the University of Birmingham MC40 cyclotron [27]. For imaging, the source was placed in a small plastic sample holder and fixed to a block of polystyrene foam at six locations ranging from the centre of the FOV and locations at 1/4th of the FOV. These locations and the source activities at the time of the experiment are listed in Table 1. The source and the LaMA geometry are shown in Fig. 2.

TABLE 1. Spatial resolution test parameters.

X (mm)	Y (mm)	Z (mm)	Initial Activity (MBq)	End Activity (MBq)
0	0	0	2.26	2.07
0	77.5	0	2.06	1.91
86.25	0	0	1.88	1.69
0	0	125	1.39	1.20
0	77.5	125	1.19	1.05
86.25	0	125	1.00	0.86

To produce projection images, the LoRs collected from the experiment were first voxelised into a three-dimensional array with a 1 mm voxel size using the voxelisation method

FIGURE 2. The spatial resolution tests are conducted using a 1 mm diameter resin bead placed inside a plastic sample holder and taped to a piece of polystyrene foam.

implemented in the `pept` Python package [28]. Two-dimensional slices from this array were extracted which contain the voxel with the maximum number of LoR crossings. From these slices. A one-dimensional profile was drawn through the maximum voxel and the FWHM was extracted from each position. Following the NEMA protocol, the spatial resolution is calculated using (1-4).

$$Res_{Trans_{Center}} = (Res_{y_{x=0,y=0,z=0}} + Res_{x_{x=0,y=0,z=0}} + Res_{y_{x=1/4,y=0,z=0}} + Res_{x_{x=1/4,y=0,z=0}})/4 \quad (1)$$

$$Res_{Trans_{1/4}} = (Res_{y_{x=0,y=1/4,z=1/4}} + Res_{x_{x=0,y=1/4,z=1/4}} + Res_{y_{x=0,y=1/4,z=0}} + Res_{x_{x=0,y=1/4,z=0}})/4 \quad (2)$$

$$Res_{Axial_{Center}} = (Res_{z_{x=0,y=0,z=0}} + Res_{z_{x=1/4,y=0,z=0}})/2 \quad (3)$$

$$Res_{Axial_{1/4}} = (Res_{z_{x=0,y=0,z=1/4}} + Res_{z_{x=1/4,y=0,z=1/4}})/2 \quad (4)$$

2) COUNT-RATE RESPONSE

The count-rate experiment measures the LoR count-rate of the detector in response to a central source which is imaged over several half-lives. The total, true, and scattered plus random LoRs count-rates are extracted using the NEMA protocol and recorded at regular intervals as a function of source activity. The scattered plus random count-rate is termed the corrupted count-rate since the LoRs do not pass through the positron annihilation point due to scattering or originating from separate annihilation events and thus are treated as noise in a PEPT experiment.

The phantom is a hollow, high-density polyethylene cylinder measuring 120 mm in height and 50 mm in diameter with an inner cavity measuring 100 mm in height by 12 mm in diameter. This cavity is filled with a well-mixed solution of fluorine-18 and water. Initially, the activity of the phantom was approximately 80 MBq. This activity was chosen such that the expected count-rate will exceed the maximum rate at which LoRs can be recorded by the detector, then, as the source decays, the count-rate response curves can be developed. The phantom was imaged over several half-lives until the activity reached near that of the background. The phantom and detector geometry are shown in Fig. 3.

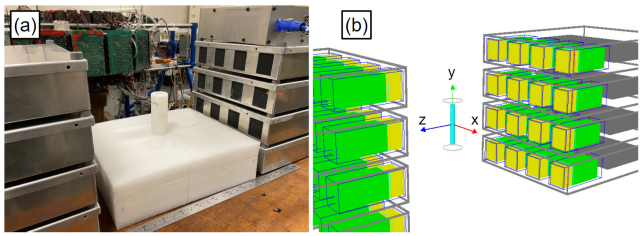

FIGURE 3. (a) The count-rate experiment is conducted with the high-density polyethylene phantom placed in the centre of FOV and imaged over several half-lives. (b) A GATE model of the same experiment is conducted.

Similarly to Section II-A1, projection images are produced by voxelising LoRs into a three-dimensional array with a 1 mm voxel size. Two-dimensional slices are extracted in the plane parallel to the detector face (XY plane) which contains the maximum voxel. The slice is then transformed into a one-dimensional profile by summing the voxels in the Y-axis which are along the cylinder's axis. The average source activity, $\bar{A}$, for each projection image is determined by (5) which calculates the average activity by using the initial activity, A_0, the initial and final time of the acquisition, t_0 and t_f, as well as the decay constant for fluorine-18, λ. The true counts are considered to be the LoRs $\pm$ 20 mm from the peak of the profile from which the background on either side of the 40 mm window is averaged and subtracted from the counts in the window. The remaining counts outside the window and including the background are considered corrupted counts.

$$\bar{A} = \frac{A_0}{t_f - t_0} \int_{t_0}^{t_f} \exp(-\lambda t)\, dt \quad (5)$$

B. GATE MODEL

The design of a GATE model for the LaMA presents several challenges since it must be easily customised to rapidly prototype new geometries, only allow specific coincidences to be formed between boxes connected to a single coincidence processor, and be able to emulate the noise, data buffer, and spatial blurring inherent in the system. Achieving these goals is accomplished using the tools available in the GATE software in addition to custom data post-processing. The geometry, digitizer, and post-processing are described in the following sections. A downloadable version of the LaMA GATE model and post-processing software is provided through a GitHub repository: LaMA Model.

1) GEOMETRY MODEL

Since any LaMA geometry is built using boxes, to build a model of the LaMA, only a single box needs to be described which can later be copied, translated, and rotated to any position and orientation using GATE's generic repeater function. The dimensions for each box are found in Section I-A and these are replicated in GATE. Material definitions for BGO, aluminium frame, and glass light guide are already included in the GATE materials database and definitions for the PMTs and electronics are added. Importantly, the four ECAT951 block detectors are included in each box and the 8 × 8 BGO crystal array in each block is defined as the 'Sensitive Detector' (SD) through which GATE records the interactions of particles. The model of a single box is shown in Fig. 4 from various viewpoints. The order in which the repeated boxes are listed determines their volume number, which will become important later when defining which pairs of boxes are valid for recording coincidences.

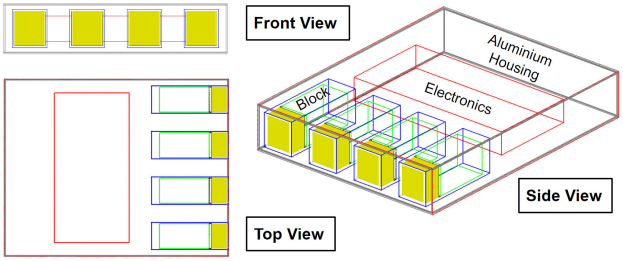

FIGURE 4. A model of a box for the LaMA consisting of four ECAT951 block detectors each with an 8 × 8 array of BGO crystals. The box is shown from various viewpoints and has major components labelled.

2) DIGITIZER MODEL

While a geometric model ensures the interactions of the source's radiation field with the detector are accurately recorded, the system's pulse-processing chain must also be properly modelled in order to emulate the detector's response. In GATE, implementing a linear pulse-processing chain to particle interactions is the role of the digitizer. The digitizer is a series of steps and filters which transform the observable information (time, energy, position) of a particle interaction with the SD into a form similar or identical to the real detector output [29]. This includes grouping interactions, flow-logic, and data-loss to mimic the real behaviour of the imaging system [30]. The digitizer for the LaMA is shown in Fig. 5.

For the LaMA, we apply a typical digitizer model for a PET system, but also implement a post-processing stage to implement aspects of the detector not directly possible through GATE [19]. This is needed to force the detector to only record coincidences between pairs of boxes which are associated with each other in the real coincidence processor, implement a random spatial-blurring of LoRs to match the experimentally observed spatial resolution, and implement a bandwidth limitation to cap the rate at which LoRs are written to file. The post-processing steps for the LaMA GATE model digitizer are the final three steps before the final simulated detector response is produced, as shown in Fig. 5.

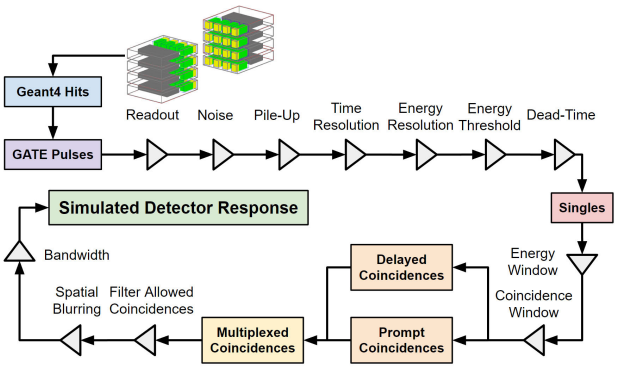

FIGURE 5. The pulse-processing digitizer of the LaMA GATE model.

C. DIGITIZER OPTIMISATION

Even if every detail of the LaMA were known, there are differences between simulation and experiment which require aspects of the digitizer to be calibrated [10], [31]. While this could be achieved through manual calibration, for this we work we use a recently developed method which applies an evolutionary algorithm to achieve a calibration to experimental performance characteristics autonomously [15].

Six stages of the digitizer are chosen to be calibrated because of the effect they have on replicating the count-rate response. These are the noise frequency, pile-up time, time resolution, lower-level energy discriminator, upper-level energy discriminator, and the non-paralysable singles dead-time. The noise frequency is the rate at which random events are generated simply by having the detectors running and is a combination of the background activity and electronic noise. The pile-up time is the time after an event is detected when other events in close succession can be added to the signal. The time resolution is the probability of precision by which two events can be distinguished in time, as defined by an FWHM. The lower and upper energy discriminators are the thresholds between which an event can trigger the dead-time and be recorded. The singles dead-time is a non-paralysable dead-time model, described by (6) which limits the rate of recording single events [32].

$$\frac{\lambda_{out}}{\lambda_{in}} = \frac{1}{(1 + \lambda_{in}\tau)} \tag{6}$$

In order to use an evolutionary algorithm to calibrate a GATE model, there must a metric through which the fitness of candidate solutions to the parameters of the digitizer can be assessed. This is achieved through a cost function, shown in (7), which is the product of the percent differences between the experiment and simulation's total, true, and corrupted count-rate response over a range of source activities, calculated using (8-10). Using this metric reduces the agreement between the experiment and simulation down to a single value

which can be optimised through minimisation of (7).

$$\varepsilon = \varepsilon_{Tot}\varepsilon_{True}\varepsilon_{Corrupt} \tag{7}$$

$$\varepsilon_{Tot} = \sum |(R_{Tot_{exp}} - R_{Tot_{sim}})/R_{Tot_{exp}}| \tag{8}$$

$$\varepsilon_{True} = \sum |(R_{True_{exp}} - R_{True_{sim}})/R_{True_{exp}}| \tag{9}$$

$$\varepsilon_{Corrupt} = \sum |(R_{Corrupt_{exp}} - R_{Corrupt_{sim}})/R_{Corrupt_{exp}}| \tag{10}$$

Parameter combinations are generated following a multivariate normal distribution with the initial uncertainty defined as the range between the upper and lower bounds of the solution space for each parameter. To stop the optimisation, the user must provide either the number of generations, called epochs, of simulations desired or provide a target uncertainty in the calibrated parameters. In this optimisation, we used 100 epochs with 100 parameter value combinations per epoch as the terminating criteria because this provides greater than 10 times the factorial of the number of free-parameters in the optimisation, sufficiently constraining the problem.

Each combination is simulated over 10 different activities, ranging from 2 MBq to 80 MBq, until 5 million LoRs are recorded at each activity. This number of LoRs provides sufficient counts such that an accurate measurement of each respective count-rate can be extracted from the projection images. The bounds of the parameters and their initial guesses are provided in Table 2. The optimisation is conducted on the University of Birmingham's high-performance computing system, BlueBEAR, on Icelake cores with 16 GB of memory each. After the optimisation is finished, the calibrated parameters are extracted and a new set of simulations are conducted with 20 activities over the same activity range until 30 million LoRs are recorded, reducing statistical error even further. These simulations are presented and compared in Section III.

TABLE 2. Digitizer parameter bounds and initial guesses for calibration.

Parameter	Lower Bound	Upper Bound	Initial Guess
Singles Dead-Time (ns)	0	10000	5000
Noise Frequency (ns)	1000	10000	5500
Pileup Time (ns)	0	1000	500
Lower Level Disc. (keV)	0	400	200
Upper Level Disc. (keV)	700	2200	1450
Time Resolution (ns)	0	30	15

III. RESULTS AND DISCUSSION

In this section, we present the results of the characterisation experiments as well as the results of the digitizer calibration. For spatial resolution, six tracer positions were imaged over several minutes then the FWHM of the 1-dimensional PSF is extracted. The FWHM at these positions are used to compute the transaxial and axial spatial resolutions in the centre of the FOV and at 1/4th of the FOV. Next, the experiments are reproduced in simulation and the crystal blurring is adjusted until the best match between the experiment and simulation was achieved. The crystal blurring that best agrees with the experiment 2 times the crystal dimensions

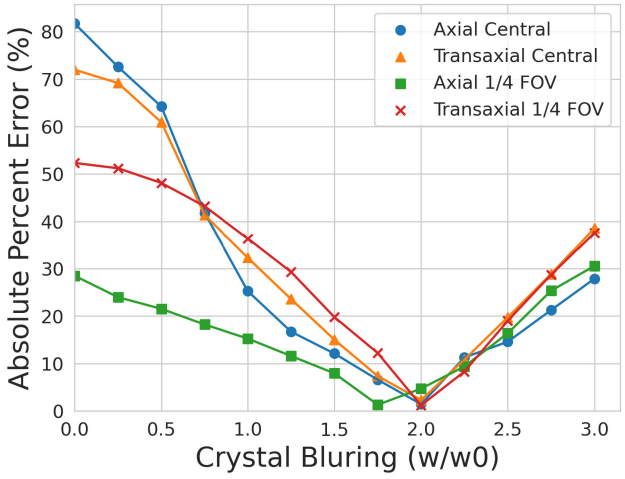

FIGURE 6. The spatial blurring is calibrated by finding the crystal blurring that minimises the absolute percent error.

TABLE 3. Results and comparisons of the spatial resolution tests for the experiment and simulation.

Spatial Resolution	Experiment (mm)	Simulation (mm)	Percent Error (%)
Central Transaxial	8.26	8.38	1.44
1/4th FOV Transaxial	8.95	9.37	4.72
Central Axial	21.83	22.34	2.32
1/4th FOV Axial	24.09	23.80	-1.20

(6.25 mm by 6.75 mm), as evidenced in Fig. 6. The experimental and simulated results are presented in Table 3 and compared through their respective percent differences.

Following the spatial resolution characterisation and crystal blurring calibration, the count-rate response experiments were analysed to be used as a comparison for the ACCES optimisation. The optimisation takes place over 100 epochs with 100 parameter value combinations tried every epoch. This results in 10,000 cost function evaluations which took approximately three days to complete running the BlueBEAR high-performance computing system. At the end of the optimisation, the final mean parameter values were extracted. The value for these parameters and their uncertainty are provided in Table 4. Additionally, the history of these parameters during the optimisation (uncertainties and mean values) is presented in Fig. 7, demonstrating that before the end of the optimisation, each parameter reaches a stable value, meaning that the parameters have been calibrated.

All parameters produced reasonable calibrations within the upper and lower bounds given to the optimiser. Interestingly, the optimised value for the time resolution falls within the 12 ns $\pm$ 2 ns measured in a previous characterisation of the LaMA [31]. This provides additional evidence that the calibrated parameters correspond to physical reality and are global solutions, not simply local solutions.

The parameter with the highest uncertainty is the upper level energy discriminator. We believe this is due to the relatively small impact of this parameter on the calibration. To illustrate this, take for example the the singles dead-time which has the lowest uncertainty. The singles dead time has

a strong pressure to be calibrated because this is applied to nearly all events which are detected. meaning small changes in the calibrated values will causes large differences in the simulated count-rate response. On the other hand, the upper energy discriminator acts on a much smaller set of events and can only be applied to events that have piled up on one another. Since the upper energy discriminator is set to 1990 keV, this means that at least four 511 keV events must be grouped together and this happens only a limited number of times in a simulation. As a result, there is not a strong pressure to calibrate this value. While this results in a higher uncertainty, because of the lower effect of this parameter on the overall response of the model this value is considered adequately calibrated.

TABLE 4. Digitizer calibration results and uncertainty.

Parameter	Calibrated Values	Uncertainty
Singles Dead-Time (ns)	6630	± 57.9
Noise Frequency (ns)	1970	± 9.39
Pileup Time (ns)	637	± 6.91
Lower Level Disc. (keV)	324	± 7.99
Upper Level Disc. (keV)	1990	± 85.5
Time Resolution (ns)	13.7	± 0.084

When the new set of simulations is conducted with the calibrated digitizer, the results match the experiment to a mean absolute difference of 3.41% over all three count-rates

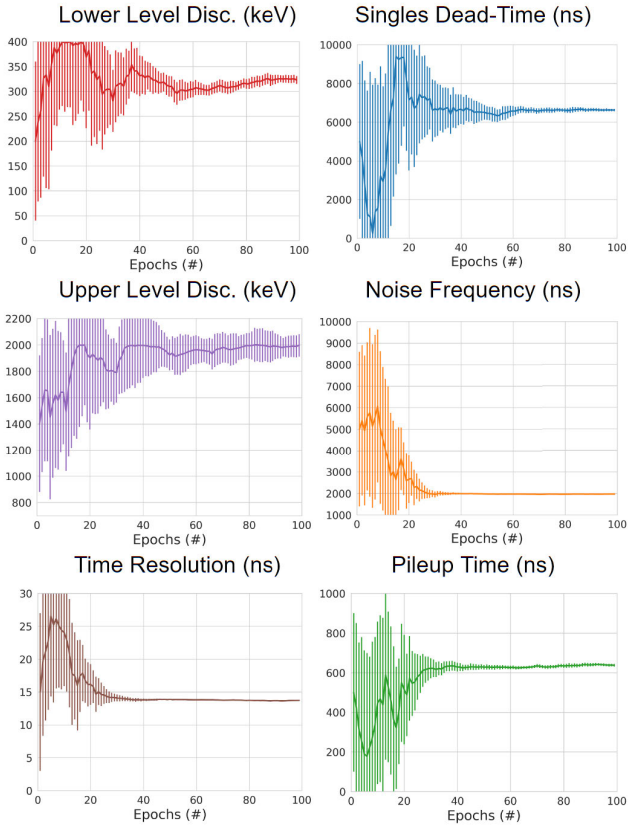

FIGURE 7. Subplots showing the mean values of calibrated parameters with the error bars as the standard deviation of solutions.

with the total, true, and corrupted count-rates being 2.31%, 2.18%, and 5.72%, respectively. The experimental and simulated count-rate response is shown in Fig. 8. To quantify the calibration further, it is also important to observe how the fraction of true and corrupted counts behave as a function of source activity. These results are presented in Fig. 9, showing that their behaviour is approximately the same overall activities with the true and corrupted count fractions reconstructed to 1.91% and 3.72% error, respectively.

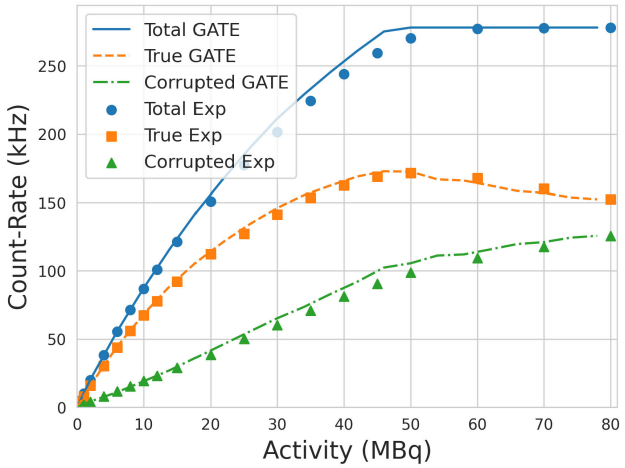

FIGURE 8. Results of the count-rate experiment and comparison of the ACCES calibrated GATE model.

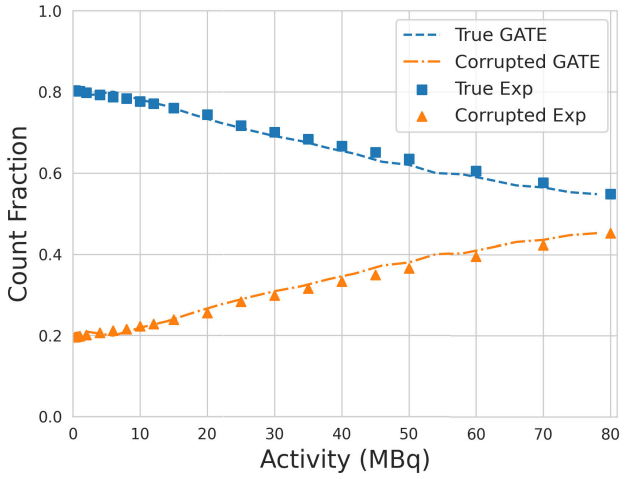

FIGURE 9. Results of the count-rate experiment in terms of the true and corrupt count fractions and comparison with the ACCES calibrated GATE model.

In summary, the GATE model of the LaMA has been characterised by experiments testing the spatial resolution and count-rate response and the digitizer pulse-pulse processing model has been calibrated using an evolutionary algorithm. In addition to calibrating the amount of crystal spatial blurring, six free-parameters of the pulse-processing digitizer model were calibrated using evolutionary simulation,

ultimately producing simulated results which match the observed real behaviour of the detector system. The ACCES software was used to perform this optimisation autonomously, needing only the number of solutions to try for each epoch, the bounds of the solution space for each parameter, and a terminating criterion.

IV. CONCLUSION

In this work, we have introduced a Monte Carlo model of the Positron Imaging Centre's LaMA and validated the model against experimental measurements. This model will bolster the modelling capabilities of the Positron Imaging Centre, complementing the existing Monte Carlo model of the ADAC Forte. A model of LaMA is particularly useful because the camera is typically configured into new geometries for every experiment in order to capture the relevant system behaviour. Prior to this model, it was not possible to quantitatively estimate the spatial resolution and count-rate response because these characteristics depend on a complex relationship between source activity, detector geometry, and gamma-ray scattering. Using this model, not only can the spatial resolution and count rate response be estimated, but moreover the tracer activity which maximises the true count-rate and the detector geometry which maximises the camera sensitivity for a given experiment can be identified.

CONFLICT OF INTEREST

The authors declare that there is no conflict of interest.

ACKNOWLEDGMENT

The authors would like to thank Andrei Nicusan for developing and maintaining the `pept` Python Library and Access Optimization Tools. The computations described in this article were performed using the University of Birmingham's BlueBEAR service, which provides High-Performance Computing to the University's research community. See their website for more details.

REFERENCES

[1] K. Windows-Yule, L. Nicusan, M. T. Herald, S. Manger, and D. Parker, *Positron Emission Particle Tracking*. Bristol, U.K.: IOP Publishing, 2022.

[2] C. R. K. Windows-Yule, J. P. K. Seville, A. Ingram, and D. J. Parker, "Positron emission particle tracking of granular flows," *Annu. Rev. Chem. Biomol. Eng.*, vol. 11, no. 1, pp. 367–396, Jun. 2020.

[3] D. J. Parker, C. J. Broadbent, P. Fowles, M. R. Hawkesworth, and P. McNeil, "Positron emission particle tracking—A technique for studying flow within engineering equipment," *Nucl. Instrum. Methods Phys. Res. A, Accel. Spectrom. Detect. Assoc. Equip.*, vol. 326, no. 3, pp. 592–607, Mar. 1993.

[4] M. Al-Shemmeri, K. Windows-Yule, E. Lopez-Quiroga, and P. J. Fryer, "Coffee bean particle motion in a spouted bed measured using positron emission particle tracking (PEPT)," *J. Food Eng.*, vol. 311, Dec. 2021, Art. no. 110709.

[5] C. R. Jones, A. Corona, C. Amador, and P. J. Fryer, "Dynamics of fabric and dryer sheet motion in domestic clothes dryers," *Drying Technol.*, vol. 40, no. 10, pp. 2087–2104, 2021.

[6] A. Dybalska, A. J. Caden, D. J. Parker, J. Wedderburn, and W. D. Griffiths, "Liquid metal flow studied by positron emission tracking," *Metall. Mater. Trans. B*, vol. 51, no. 5, pp. 1912–1917, Oct. 2020.

[7] D. J. Parker, D. M. Hampel, and T. K. Wheldon, "Performance evaluation of the current Birmingham PEPT cameras," *Appl. Sci.*, vol. 12, no. 14, p. 6833, Jul. 2022.

[8] D. Parker, R. Forster, P. Fowles, and P. Takhar, "Positron emission particle tracking using the new Birmingham positron camera," *Nucl. Instrum. Methods Phys. Res. A, Accel. Spectrom. Detect. Assoc. Equip.*, vol. 477, nos. 1–3, pp. 540–545, Jan. 2002.

[9] D. M. Hampel, S. Manger, D. J. Parker, and T. K. Wheldon, "SuperPEPT: A new tool for positron emission particle tracking; first results," *Nucl. Instrum. Methods Phys. Res. A, Accel. Spectrom. Detect. Assoc. Equip.*, vol. 1028, Apr. 2022, Art. no. 166254.

[10] D. J. Parker, T. W. Leadbeater, X. Fan, M. N. Hausard, A. Ingram, and Z. Yang, "Positron emission particle tracking using a modular positron camera," *Nucl. Instrum. Methods Phys. Res. A, Accel. Spectrom. Detect. Assoc. Equip.*, vol. 604, nos. 1–2, pp. 339–342, Jun. 2009.

[11] W. D. Griffiths, D. J. Parker, X. Fan, and M. Hausard, "Tracking inclusions in aluminium alloy castings using positron emission particle tracking (PEPT)," *Mater. Sci. Technol.*, vol. 26, no. 5, pp. 528–533, May 2010.

[12] S. Jan et al., "GATE: A simulation toolkit for PET and SPECT," *Phys. Med. Biol.*, vol. 49, no. 19, pp. 4543–4561, Oct. 2004.

[13] D. Sarrut et al., "Advanced Monte Carlo simulations of emission tomography imaging systems with gate," *Phys. Med. Biol.*, vol. 66, no. 10, May 2021, Art. no. 10TR03.

[14] *Performance Measurements of Positron Emission Tomographs (PET) 2018*, National Electrical Manufacturers Association, Rosslyn, VA, USA, 2018.

[15] M. Herald, A. Nicuşan, T. K. Wheldon, J. Seville, and C. Windows-Yule, "Autonomous digitizer calibration of a Monte Carlo detector model through evolutionary simulation," *Sci. Rep.*, vol. 12, no. 1, p. 19535, Nov. 2022.

[16] N. Hansen, K. Nozawa, L. Rolshoven, M. Chan, Y. Akimoto, and D. Brockhoff, "CMAES/pycma: R3.2.2," Zenodo, Tech. Rep., Mar. 2022.

[17] A.-L. Nicusan, D. Werner, J. A. Sykes, J. Seville, and K. Windows-Yule, "ACCES: Autonomous characterisation and calibration via evolutionary simulation," GitHub, San Francisco, CA, USA, Tech. Rep., Feb. 2022.

[18] M. Herald, T. Wheldon, and C. Windows-Yule, "Monte Carlo model validation of a detector system used for positron emission particle tracking," *Nucl. Instrum. Methods Phys. Res. A, Accel. Spectrom. Detect. Assoc. Equip.*, vol. 993, Mar. 2021, Art. no. 165073.

[19] S. Lee, J. Gregor, and D. Osborne, "Development and validation of a complete GATE model of the Siemens Inveon trimodal imaging platform," *Mol. Imag.*, vol. 12, no. 7, Oct. 2013, Art. no. 7290.2013.00058.

[20] M. Herald, Z. Bingham, R. Santos, and A. Ruggles, "Simulated time-dependent data to estimate uncertainty in fluid flow measurements," *Nucl. Eng. Des.*, vol. 337, pp. 221–227, Oct. 2018.

[21] C. R. K. Windows-Yule, M. T. Herald, A. L. Nicusan, C. S. Wiggins, G. Pratx, S. Manger, A. E. Odo, T. Leadbeater, J. Pellico, R. T. M. D. Rosales, A. Renaud, I. Govender, L. B. Carasik, A. E. Ruggles, T. Kokalova-Wheldon, J. P. K. Seville, and D. J. Parker, "Recent advances in positron emission particle tracking: A comparative review," *Rep. Prog. Phys.*, vol. 85, no. 1, Jan. 2022, Art. no. 016101.

[22] M. T. Herald, J. A. Sykes, D. Werner, J. P. K. Seville, and C. R. K. Windows-Yule, "DEM2GATE: Combining discrete element method simulation with virtual positron emission particle tracking experiments," *Powder Technol.*, vol. 401, Mar. 2022, Art. no. 117302.

[23] S. Shalev-Shwartz, O. Shamir, and S. Shammah, "Failures of gradient-based deep learning," in *Proc. 34th Int. Conf. Mach. Learn.*, vol. 70, D. Precup and Y. W. Teh, Eds., Aug. 2017, pp. 3067–3075.

[24] M. Strugari, D. DeBay, S. Beyea, and K. Brewer, "NEMA NU 1–2018 performance characterization and Monte Carlo model validation of the Cubresa Spark SiPM-based preclinical SPECT scanner," *EJNMMI Phys.*, Aug. 2022.

[25] A. Tiwari, M. Merrick, S. A. Graves, and J. Sunderland, "Monte Carlo evaluation of hypothetical long axial field-of-view PET scanner using GE discovery MI PET front-end architecture," *Med. Phys.*, vol. 49, no. 2, pp. 1139–1152, Feb. 2022.

[26] Y. Kwon, S. Kang, Y.-S. Choi, and I. Kim, "Evolutionary design of molecules based on deep learning and a genetic algorithm," *Sci. Rep.*, vol. 11, no. 1, p. 17304, Aug. 2021.

[27] D. J. Parker, "Positron emission particle tracking and its application to granular media," *Rev. Sci. Instrum.*, vol. 88, no. 5, May 2017, Art. no. 051803.

[28] A. L. Nicuşan and C. R. K. Windows-Yule, "Positron emission particle tracking using machine learning," *Rev. Sci. Instrum.*, vol. 91, no. 1, Jan. 2020, Art. no. 013329.
[29] S. Kerhoas-Cavata and D. Guez, "Modeling electronic processing in GATE," *Nucl. Instrum. Methods Phys. Res. A, Accel. Spectrom. Detect. Assoc. Equip.*, vol. 569, no. 2, pp. 330–334, Dec. 2006.
[30] D. Guez, F. Bataille, C. Comtat, P.-F. Honore, S. Jan, and S. Kerhoas, "Counting rates modeling for PET scanners with GATE," *IEEE Trans. Nucl. Sci.*, vol. 55, no. 1, pp. 516–523, Feb. 2008.
[31] T. W. Leadbeater, "The development of positron imaging systems for applications in industrial process tomography," Ph.D. thesis, Univ. Birmingham, Birmingham, U.K., Jul. 2009.
[32] S. Usman and A. Patil, "Radiation detector deadtime and pile up: A review of the status of science," *Nucl. Eng. Technol.*, vol. 50, no. 7, pp. 1006–1016, Oct. 2018.

MATTHEW HERALD was born in the USA. He received the B.S. degree in nuclear engineering from the University of Tennessee, Knoxville, in 2019. He is currently pursuing the Ph.D. degree in chemical engineering with the University of Birmingham, under the supervision of Christopher Windows-Yule.

He is a member of the Institue of Physics and currently works for Jacobs as a Physicist. His work revolves around developing Monte Carlo models of position-sensitive detectors and simulating positron emission particle tracking experiments to optimize data acquisition. He has developed a model of the ADAC Forte dual-headed positron camera and used this in an international collaboration of other institutes using positron emission particle tracking algorithms to benchmark their performance on a common, known data set. He is the coauthor on the first book written about positron emission particle tracking which was written to be used by students, users, and researchers.

DAWID HAMPEL was born in Poland, but spent most of his primary education in the USA. He received the M.Eng. degree (Hons.) in nuclear engineering from the University of Birmingham, Birmingham, U.K., in 2019, where he is currently pursuing the Ph.D. degree in cyclotron production and radiochemical purification methods of emerging radionuclides for cancer diagnosis and treatment while developing positron emission particle tracking detector arrays.

His early work includes the development of Geant4 radiation transport simulations and simulations of numerous nuclear reactions in TALYS and EMPIRE. He is the Co-Developer of UoB-TIP Toolkit used to ease the analysis of nuclear reaction data and OLab an online, interactive nuclear laboratory both used with the University of Birmingham. His current work involves the development and improvement of PEPT detector arrays in both hardware and software levels. He is working with the Positron Imaging Centre, he has built and tested SuperPEPT and redeveloped and modernized the Large Modular Array (LaMA) for PEPT with contributions to other systems used at the site.

Mr. Hampel is a member of the Institute of Physics.

TZANY KOKALOVA WHELDON received the Ph.D. degree in nuclear physics from Freie Universitaet, Berlin, Germany.

She is currently a full-time Professor of nuclear physics with the University of Birmingham and the Director of the Positron Imaging Centre. Her work spans the full breadth of nuclear physics from experimental nuclear astrophysics and machine learning, medical isotopes, applications, and industry-related nuclear decommissioning. She carries out research, teaches, and supervises eight Ph.D. students, and key roles mentoring women. She has travelled extensively, performing experiments with laboratories in Australia, the USA, and Europe. She was a recipient of the Daphne Jackson Fellowship and won a Timewise Power Returner Award celebrating, in 2020, her ability to combine career success at a senior level whilst working flexibly.

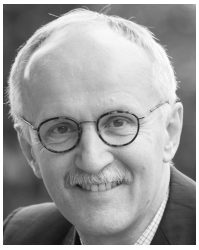

JONATHAN SEVILLE was born in Yorkshire, U.K. He received the degree in chemical engineering from the University of Cambridge and University of Surrey.

Before starting his academic career, he worked for several years for the research division of Courtaulds Ltd. Since 2017, he has been a Professor of formulation engineering with the University of Birmingham. Previously, he was the Executive Dean of Engineering and Physical Sciences with the University of Surrey (2011–2016), the Dean of Engineering with the University of Warwick (2008–2011), and the Head of the Department of Chemical Engineering, University of Birmingham (1998–2008). He is an experienced researcher in chemical engineering, particularly in processes involving particulate solids, and has pioneered the use of radioactive tracers to image flow in industrial equipment. He has around 200 publications and authored or edited five books on aspects of particle technology. Among the numerous companies which have supported his research are Unilever, Procter and Gamble, GSK, Merck Sharp and Dohme, and Pfizer. He is a fellow of the Royal Academy of Engineering and was President of the Institution of Chemical Engineers (IChemE), in 2016–2017.

CHRISTOPHER WINDOWS-YULE was born in Worcestershire. He received the B.S. and Ph.D. degrees in physics from the University of Birmingham.

Previously, he was a Postdoctoral Researcher with the University of Twente, The Netherlands. He is currently an Associate Professor with the University of Birmingham's School of Chemical Engineering. His research interests include imaging and numerical modeling of particulate and multiphase systems, employing a diverse range of techniques, notably discrete element method (DEM) modeling, computational fluid dynamics (CFD), and positron emission particle tracking (PEPT). His research aims to address significant contemporary challenges in science, medicine and industry by exploiting the synergy of experimental techniques, numerical simulation, and machine-learning methodologies. His current projects include work, funded by EPSRC, the Royal Academy of Engineering and the Royal Society, developing novel plastic recycling methods, work funded by the British Heart Foundation aiming to develop novel methods of blood-flow imaging for the diagnosis of cardiovascular disease, and diverse industry-funded projects. He is a Turing Fellow, a two-time Royal Academy of Engineering Industrial Fellow, and a Founding Member of the U.K. Young Academy.